Optimal design of aluminium axial compression member with square hollow sections through a practical method

W Su, J Wang, H Wu, J Hu

TECHNICAL PAPER

JOURNAL OF THE SOUTH AFRICAN INSTITUTION OF CIVIL ENGINEERING

ISSN 1021-2019 (print) | ISSN 2309-8775 (online)

Vol 68 No 1, March 2026, Pages 31–39, Paper 1689

Aluminium columns are generally designed with hollow cross-sectional and thin-walled shapes to resist overall buckling under axial compression. Moreover, internal stiffeners are often added to column walls to improve local buckling resistance. However, only a few studies have been conducted to determine the optimal number of internal stiffeners. This study proposes a simple and practical formulation to optimally design aluminium axial compression members with internal stiffeners and assess the influence of the number of stiffeners. The objective was to minimise the weight of members to prevent the four main failure modes: yielding, overall flexural buckling, local buckling of member walls, and local buckling of internal stiffeners. The method was verified through existing experimental results from the literature. The results showed that when the number of internal stiffeners increased, the minimum weight decreased or increased by more than 20% compared to that of the columns without internal stiffeners. This indicates that there is no universal monotonicity on the number of stiffeners, and it is difficult to predict the optimal number of stiffeners using simple parameters, such as the slenderness ratio of columns and width-to-thickness ratios. Thus, the proposed optimisation method is recommended for design of aluminium compression members with internal stiffeners.

Keywords: Aluminium alloy, local buckling, optimal design, square hollow section (SHS), internal stiffeners

INTRODUCTION

Aluminium alloys have become essential structural materials in modern life owing to their versatile properties, such as light weight, corrosion resistance, ease of formation, non-toxicity, durability, and recyclability. In fact, approximately 25% of the total aluminium production worldwide is used in construction (Georgantzia 2021). Aluminium alloys can be easily extruded to produce complex and aesthetically attractive cross-sectional shapes that are frequently used as the skeletons and façades of prominent buildings. However, the elastic modulus of aluminium alloys, which is approximately 70 GPa, is only one-third of steel (The Aluminium Association 2020).

One way to improve the stiffness of aluminium alloy structural elements is to design and fabricate aluminium components with large moments of inertia in order to resist large axial compression and bending (Tsavdaridis *et al* 2019). Aluminium structural components are therefore usually designed with thin-walled hollow cross sections. The commonly employed sections include rectangular hollow sections (RHS) (Wang *et al* 2018), square hollow sections (SHS) (Feng *et al* 2018), circular hollow sections (CHS) (Feng *et al* 2016), I-sections (Wang *et al* 2018), angles (Wang *et al* 2016), channels (Zhu *et al* 2019), and some irregular sections (Tsavdaridis *et al* 2019). These cross sections significantly improve the bending stiffness and overall buckling resistance of the aluminium bars compared with the solid sections. However, local buckling of hollow aluminium structures is usually dominant in stub columns.

Numerous experimental and numerical studies relating to the local buckling of hollow aluminium structures have been conducted. For instance, Su *et al* (2014; 2017) experimentally and numerically studied the local buckling of aluminium alloy columns with RHS and SHS under axial compression

W Su, J Wang, H Wu, J Hu. Optimal design of aluminium axial compression member with square hollow sections through a practical method. J. S. Afr. Inst. Civ. Eng. 2026:68(1), Art. #1689, 9 pages. http://dx.doi.org/10.17159/2309-8775/2026/v68n1a3

PROF WENZHENG SU is a professor at the School of Transportation Engineering, Dalian Jiaotong University and a Visiting Researcher at the State Key Laboratory of Structural Analysis, Optimization and CAE Software for Industrial Equipment, Dalian University of Technology, China. His research focuses on multidisciplinary optimisation of structures and mechanical analysis of structural systems.

Contact details:
School of Transportation Engineering
Dalian Jiaotong University
Dalian 116028, China
State Key Laboratory of Structural Analysis
Optimization and CAE Software for Industrial Equipment
Dalian University of Technology
Dalian 116024, China
wzhsu@djtu.edu.cn

JIACHEN WANG is a master's student at the School of Transportation Engineering, Dalian Jiaotong University, China. His research focuses on multidisciplinary optimisation of structures.

Contact details:
School of Transportation Engineering
Dalian Jiaotong University
Dalian 116028, China
18253559187@163.com

HAOTIAN WU is a master's student at the School of Transportation Engineering, Dalian Jiaotong University, and works at Chongqing Station, Railway Chengdu Bureau, China. His research focuses on structural buckling analysis and design.

Contact details:
School of Transportation Engineering
Dalian Jiaotong University
Dalian 116028, China
Chongqing Station
Railway Chengdu Bureau
Chongqing 610082, China
1204418683@qq.com

PROF JINXIU HU is an Associate Professor in the School of Transportation Engineering, Dalian Jiaotong University, China. Her research focuses on computational solid mechanics and numerical analysis and simulation.

Contact details:
School of Transportation Engineering
Dalian Jiaotong University
Dalian 116028, China
hujinxiu@djtu.edu.cn

and bending. Feng and co-authors (Feng *et al* 2018; Feng & Liu 2019; Feng *et al* 2020) conducted a series of investigations on aluminium perforated columns with hollow sections of different shapes, and concluded that local buckling is a common failure mode for these structures. Liu *et al* (2015a; 2015b) tested the local buckling behaviours of aluminium stub columns with irregular hollow sections. In addition, the local and overall buckling failures and their interaction in aluminium columns with angles and I-shaped sections, and channel sections with different slenderness ratios, were investigated by Wang *et al* (2016; 2017) and Zhu *et al* (2019), respectively. The aforementioned studies confirmed that local buckling is a dominant failure mode for aluminium stub columns with hollow sections.

The addition of internal stiffeners to the hollow sections is a common method for improving the local buckling resistance of stub columns (Timoshenko & Gere 1963). The terminology "stiffener" denotes elements with the full length of a compression member to improve strength; hence, each cross section over the full length has the same geometry. Su *et al* (2014) conducted a test series on aluminium alloy stub columns having RHS and SHS, with and without internal cross stiffeners. The results showed an interesting phenomenon: some of the columns with the same dimensions exhibited a similar load-bearing efficiency in both the presence and absence of internal cross stiffeners. For example, the column with internal stiffeners labelled as +H120×70×10.5C possessed a cross-sectional area of 5 854 mm^2 and failure compression resistance of 1 164.3 kN; while the column without internal stiffeners labelled as H120×70×10.5C possessed a cross-sectional area of 3 944 mm^2 and failure compression resistance of 862.5 kN. The amount of material of the latter was 1.48 times the former, and the failure compression of the latter was 1.35 times the former. Hence, the load-bearing efficiencies of the columns with and without internal stiffeners were similar. An interesting issue was then identified: whether the addition of internal stiffeners actually improves the load-bearing efficiency of columns, and how to obtain an optimal design of a hollow column with internal stiffeners. Intuitively, the load-bearing capacity of aluminium columns should be influenced by the size, number, and even the existence of internal stiffeners. However, the mechanism of these influences on the load-bearing capacity remains to be investigated.

Generally, the design of SHS columns is conducted through design codes or numerical optimisation methods. However, neither method suits the design of SHS columns with internal cross stiffeners. It is difficult to find available solutions in the existing codes for complex structures. Furthermore, the existing codes rarely provide the details of the requirement and optimal number of internal stiffeners. In addition, the accuracy of design codes is frequently not satisfied. Therefore, the accuracy of the design codes is frequently unsatisfactory, and use of these codes requires the expertise and experience of engineers. In contrast, numerical optimisation can theoretically provide accurate solutions for complex structures. However, numerical optimisation methods are mostly combined with the finite element method. It is necessary to discretise the bar using numerous elements to obtain a satisfactory accuracy. Hence, the computational cost is significantly higher, particularly for the analysis of members with internal stiffeners and large lengths. Therefore, a practical design method that can combine sufficient practice and satisfactory computational accuracy is needed.

In this study, a simple and practical optimal design formulation for aluminium alloy SHS compression members with internal cross stiffeners was established to investigate the influence of stiffeners on the load-bearing efficiency of columns. In this formulation, the load-bearing efficiency of columns that were prevented from undergoing the four main failure modes was assessed by their weights. These four failure modes were as follows: yielding, overall flexural buckling, and local buckling of the column walls and internal stiffeners, if they existed. The design variables included the thicknesses of the column faces and internal stiffeners, and the number of stiffeners. If the number of stiffeners in an optimal design was zero, then no internal stiffeners were required. The results showed that the number of internal stiffeners played an important role in the optimal design of aluminium axial compression members with the best load-bearing efficiency. Moreover, the influence was not uniform, but dependent on the failure modes of the designed members. Furthermore, the load-bearing efficiency was improved with an increasing number of stiffeners if the member failed in local buckling; whereas an increase in the number of stiffeners reduced the efficiency if the member failed in overall flexural buckling. Notably, increasing the number did not affect the load-bearing efficiency if the column failed at yielding. Most important, increasing the number of stiffeners frequently changed the failure modes of the columns. Hence, the minimal weight of the compression members was usually non-monotonic with respect to the number of internal stiffeners. Thus, the proposed method can be used in the optimal design of aluminium columns with SHS.

OPTIMAL DESIGN MODEL

Problem statement

To determine the requirement, number, and optimal thickness of the internal stiffeners for an SHS aluminium alloy column, an optimisation model is proposed in this study. One of the considered columns is shown in Figure 1. The side length of the square box section is represented by H, while the thickness of the thin walls of the box section is t_f. The thickness of the internal stiffeners (t_c) is assumed to be constant for simplification. The number of internal stiffeners is denoted by a parameter n as $n \times n$ (as shown in Figure 1 where n = 2, and the number of stiffeners is 2×2). In addition, the internal stiffeners were assumed to be uniformly distributed in the cross section. Hence, the distance between adjacent stiffeners, h, was approximately defined as $h = H/(n+1)$, where t_c and t_f were assumed to be much smaller than h. The length of the column is denoted by L.

For simplicity, the face and internal stiffeners were both made of the same grade of aluminium alloy having density ρ, Young's modulus E, Poisson's ratio ν, and yielding strength σ_Y.

The cross-sectional geometric properties of the SHS column having $n \times n$ uniformly distributed internal stiffeners, the area A and moment of inertia about the neutral axis I, were computed as follows:

$$A = 4Ht_f + 2nHt_c \tag{1}$$

$$I = I_f + I_c \tag{2}$$

$$I_f = \frac{Ht_f^3}{6} + \frac{2t_fH^3}{3} \tag{3}$$

$$I_c = \frac{n}{12}H^3t_c + \frac{n}{12}Ht_c^3 + \frac{H^3t_c}{4(n+1)^2}\sum_{i=1}^{n}(n+1-2i)^2 \tag{4}$$

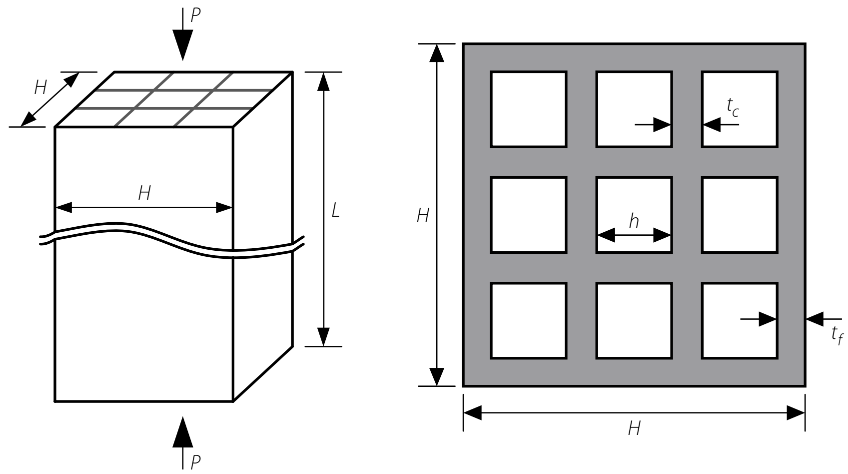

(a) Member subjected to axial compression, *P*

(b) Geometry and notations of the cross-section

Figure 1 Illustration of an SHS aluminium alloy column with internal cross stiffeners

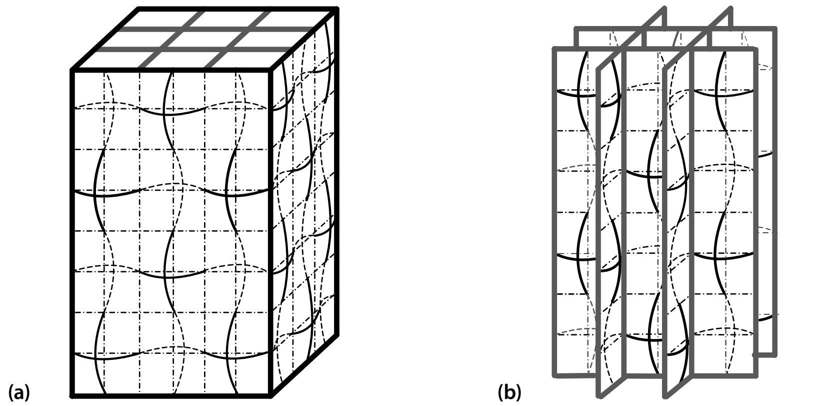

Figure 2 Illustration of local buckling modes of SHS with 2×2 internal stiffeners for (a) walls and (b) stiffeners

It should be noted that t_c and t_f were much smaller than H. Because the corners of the cells were counted twice, the geometric properties were overestimated; however, these overestimations were insignificant and thus neglected.

In this study, structural optimisation methods were adopted to obtain the optimal cross-sectional structures of the SHS aluminium alloy members. A complete optimisation model must contain an objective function, constraint functions, and design variables (Roux *et al* 1994; Arora 2017). The objective function was selected to minimise weight W of the compression member, as shown in Equation 5:

$$W = \rho AL = 2\rho LH(2t_f + nt_c) \tag{5}$$

The design variables included t_f, t_c, and n. Note that n denotes the number of stiffeners.

The main constraint functions of the present structural optimisation model were based on the assumption that none of the four common possible failure modes (yielding, overall flexural buckling, and local buckling of column walls and internal stiffeners) occurred when the member was subjected to axial compression under small deformation. These failure modes were also considered in the prior studies (Budiansky 1999; Tian & Lu 2004; Tian & Lu 2005). The local buckling of the column walls and stiffeners are shown in Figure 2 (a) and (b), respectively.

The torsional buckling and torsional flexural buckling failure modes of a general member under axial compression were not considered in this study. The present SHS member, having a closed doubly symmetric cross section, is not likely to undergo either of these by virtue of its cross-sectional geometry and, therefore, torsional rigidity. (Yu *et al* 2020; Jerath 2021). However, for a member with a general open cross section, all buckling failure modes would be considered (Tian & Lu 2004).

In addition, two size constraints on the allowable thicknesses of compression member walls and stiffeners should be included because excessively thin walls from the extrusion processes of aluminium alloy inevitably increase the defect rate of structures. Hence, it must be ensured that all thicknesses are larger than the minimum allowable thickness as follows:

$$t_f \geq \underline{t}_f,\ t_c \geq \underline{t}_c \tag{6}$$

Where $\underline{t}_f$ and $\underline{t}_c$ denote the minimum allowable thicknesses of the member walls and internal stiffeners, respectively.

In summary, the present optimisation scheme aims to find the optimal and manufacturable aluminium SHS compression members with an appropriate number of internal stiffeners to provide the best load-bearing efficiency.

Four constraints based on failure modes

As mentioned earlier, the main constraint functions are based on the common failure modes of axial compression members: yielding, overall flexural buckling, local buckling of the column walls and internal stiffeners.

Yielding

To avoid yielding of both column faces and internal stiffeners of columns, the normal stress on the cross section must satisfy the following:

$$\sigma = \frac{P}{A} \leq \sigma_Y \tag{7}$$

Where σ denotes the normal stress on the cross-section, P denotes the axial force, and σ_Y denotes the yielding stress of the aluminium alloy.

Overall flexural buckling

To avoid overall flexural buckling, the normal stress on the cross section of the SHS column must satisfy the following relationship:

$$\sigma \leq \sigma_{Eu} \tag{8}$$

Where σ_{Eu} denotes the critical stress that corresponds to the Euler buckling of a column.

The Euler stress is expressed as

$$\sigma_{Eu} = \frac{\pi^2 EI}{(KL)^2 A} \tag{9}$$

Where I denotes the moment of inertia of the column (Equations 2 to 4) and A denotes the cross-sectional area of the SHS column (Equation 1). Parameter K depends on the restrained types of the two ends of the member. In this study, for simplicity, the member was assumed to be pinned at both ends. Therefore, $K = 1$.

Hence, the constraint function of the overall buckling was expressed as

$$\frac{P}{A} \leq \frac{\pi^2 EI}{(KL)^2 A} \tag{10}$$

Local buckling of the column walls and stiffeners

The local buckling modes of the column walls and stiffeners (Figure 2) were determined by the support types of the vertical edges of the panels and their slenderness ratios. Because the stiffeners were uniformly distributed, each panel, whether a column wall or a stiffener, belongs to a basic square grid element (Figure 1). The local buckling stress of such a type of panel can be determined using the solutions of the standard problem of the hollow square columns suggested by Timoshenko and Gere (1963) as follows:

$$\sigma_f = \frac{\pi^2 E}{12(1-\nu^2)}\left(\frac{t_f}{h}\right)^2 k_f \tag{11}$$

$$\sigma_c = \frac{\pi^2 E}{12(1-\nu^2)}\left(\frac{t_c}{h}\right)^2 k_c \tag{12}$$

Where the coefficients k_f and k_c depend on the vertical boundary conditions of the face and stiffener walls; E and ν denote the Young's modulus and Poisson's ratio of the material of the member, respectively. Timoshenko and Gere (1963) indicated that the vertical boundary conditions of each panel should be considered as simply supported for SHS columns having uniform thickness, with no moments at the corners. Therefore, k_f or k_c should be 4. However, in this study, a sub-panel may have adjacent panels with non-uniform thicknesses, and the panel is neither simply supported nor clamped. Instead, it exists in between the two states. Here, it is assumed that the column length was much larger than the cell size (L/h >10); hence, k_f and k_c values should be equal to 4 or 6.97, for simply supported and clamped constraints, respectively. To obtain a conservative design, the vertical edges were considered to be simply supported; hence, $k_f = k_c = 4$.

To avoid the local buckling of column and stiffener walls, the normal stress on the cross section of the SHS column must satisfy the following relationships:

$$\sigma \leq \sigma_f \tag{13}$$

$$\sigma \leq \sigma_c \tag{13}$$

They are expressed as following relationships by substituting Equations 11 and 12 in Equations 13 and 14, respectively:

$$\frac{P}{A} \leq \frac{\pi^2 E}{12(1-\nu^2)}\left(\frac{t_f}{h}\right)^2 k_f \tag{15}$$

$$\frac{P}{A} \leq \frac{\pi^2 E}{12(1-\nu^2)}\left(\frac{t_c}{h}\right)^2 k_c \tag{16}$$

Optimisation model

Finally, the optimisation model, which was aimed at minimising weight W with respect to geometric variables t_f and t_c, and integer variable n, and subjected to the constraints in Equations 7, 10, 15, and 16, was formulated as follows:

find: t_c, t_f

min: $W = 2\rho LH(2t_f + nt_c)$

s.t.: $g_1 = 1 - \frac{A}{P}\sigma_Y \leq 0$ (yielding)

$$g_2 = 1 - \frac{\pi^2 EI}{PI^2} \leq 0 \text{ (global bucking)} \tag{17}$$

$$g_3 = 1 - \frac{\pi^2 k_f EA}{12(1-\nu^2)P}\left(\frac{t_f}{h}\right)^2 \leq 0$$

(local buckling of column walls)

$$g_4 = 1 - \frac{\pi^2 k_c EA}{12(1-\nu^2)P}\left(\frac{t_c}{h}\right)^2 \leq 0$$

(local buckling of stiffeners)

$t_f \geq \underline{t}_f$, $t_c \geq \underline{t}_c$

(allowable size constraints for manufacturers)

Where g_1, g_2, g_3, and g_4 denote the yielding constraint, overall Euler constraint, local buckling constraint of the column faces, and buckling constraint of the internal stiffeners, respectively. The aforementioned four constraint functions were normalised into a convenient form to solve the optimisation problem.

It should be noted that n does not explicitly appear in the optimisation formulation as shown in Equation 17. A simple enumeration method was used to deal with n in the optimisation model because the feasible number of the variable is finite. Based on the authors' experience, a larger n always reduces t_f and t_c to achieve the allowable thickness. Hence, the feasible n usually belongs to the internal range between of 0 and 4. The computation cost is significantly low; hence, the enumeration method is feasible and practical here.

The optimisation problem presented in Equation 17 can be solved simply using the graphical solution process because it has only two design variables, which are t_f and t_c, as expressed in the optimisation model (Equation 17). Figure 3 shows a common solution procedure for an optimisation problem. A $t_c - t_f$ coordinate system was first set up in the graph as shown in Figure 3. Each boundary of the constraint functions presented in Equation 17 was then plotted in the coordinate system, representing the points that satisfy the constraint as an equality $g_i = 0$. The constraints that satisfy equality are usually called active constraints. Points on one side of the curve satisfied the constraint function $g_i \leq 0$, and were named as feasible points, while points on the other side violate the constraint and were named as unfeasible points. After the constraint functions were all plotted, the feasible region can be obtained in which all points satisfy the total constraint functions. Here, the feasible region is the area enclosed by the thick solid green lines in the upper right corner.

Next, the contours of the objective function were plotted through the feasible region. An objective contour is a curve that connects all points with the same objective function values for given t_c and t_f. Finally, the optimum point for the optimisation problem can be located. Here, the objective contour is a family of parallel lines because the objective function is linear with respect to t_c and t_f, as shown in Equation 5. Hence, the optimal solution must appear at the boundary of the feasible region, as shown in Figure 3. For more detailed description of the graphical solution process, refer to Arora (2017).

The optimal solution(s) can be directly selected from the diagrams that contain the constraint functions and contours of the objective function. Figure 3 shows that only one unique optimal solution is available, where the overall flexural buckling

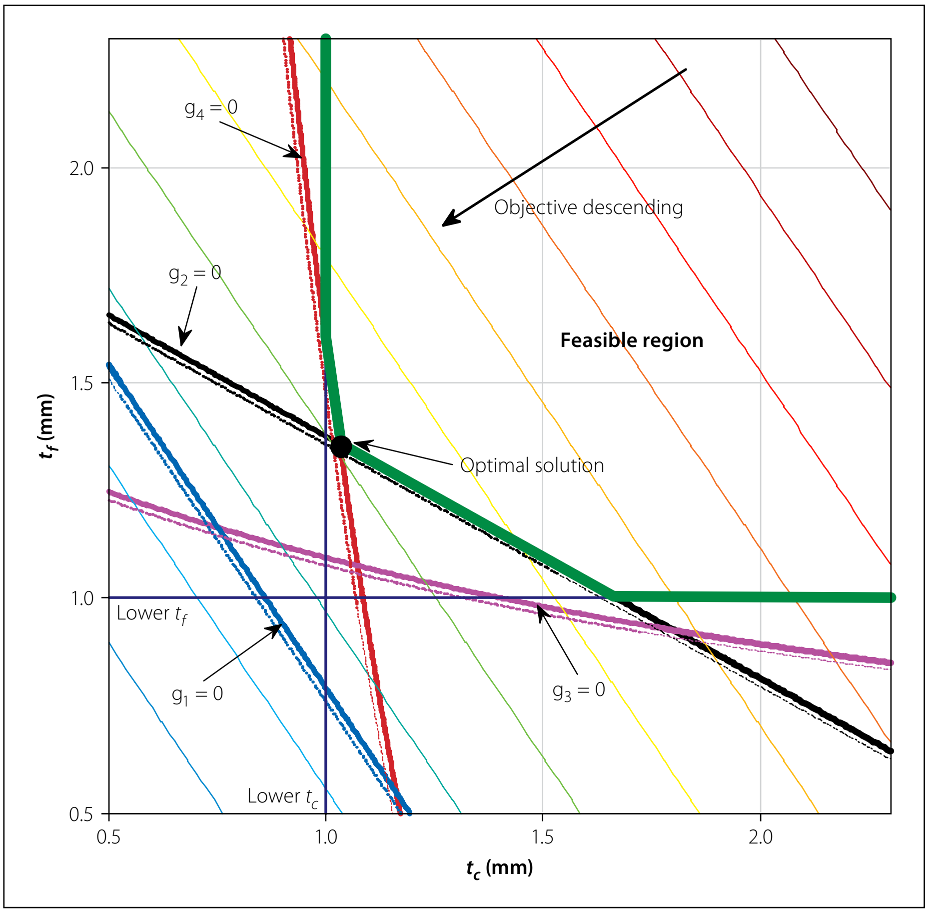

Figure 3 **Sketch of the graphic solution to an optimisation problem. The area enclosed by the green thick solid lines in the upper right corner is the feasible region**

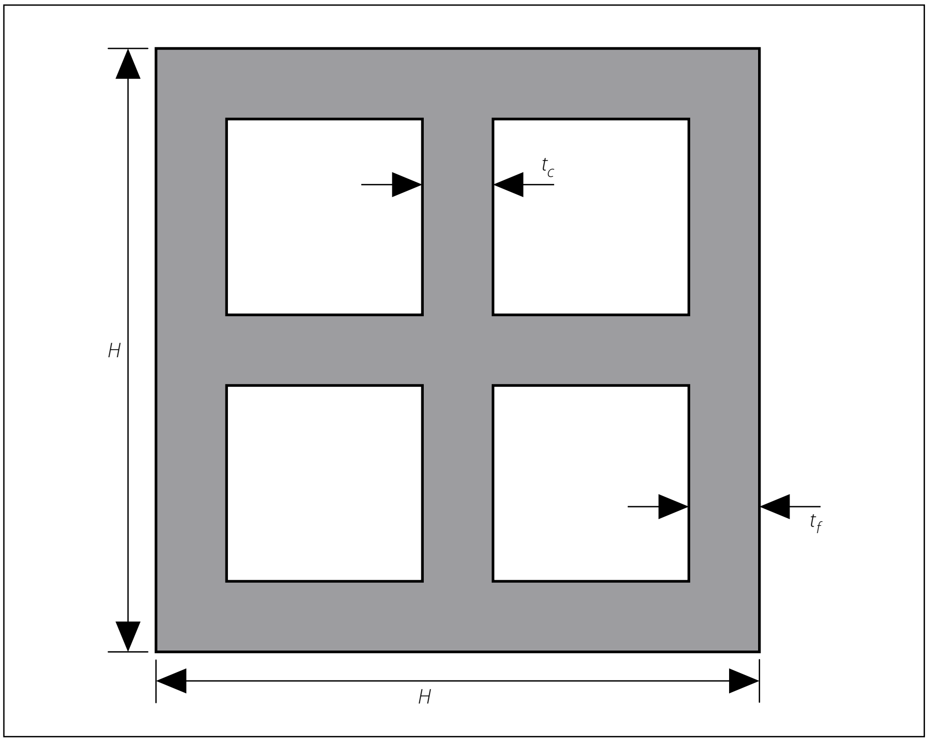

Figure 4 **Cross section with internal stiffeners of compression members shown in Su *et al* (2014)**

and local buckling of the stiffeners occur simultaneously. The values of t_c and t_f can be obtained by solving the simultaneous equations $g_2 = 0$ and $g_4 = 0$. However, an easier method is to directly select the data through a plotting software. For instance, the corresponding point in this case represented t_c = 1.03 mm and t_f = 1.36 mm. The minimum weight of the column is then computed by substituting t_c and t_f to the objective function W (Equation 5). Failure modes were identified based on the active constraints. Hence, this member failed in both overall flexural buckling and core local buckling, as shown in Figure 3. All optimisation problems in this study were solved in this manner.

RESULTS AND DISCUSSION

As mentioned earlier, the objective of this study was to propose a simple and practical method to obtain the optimal design of aluminium SHS compression members with internal stiffeners and assess the influence of the existence as well as the number of stiffeners on the load-bearing capacity. The optimisation formulation established in the 'Optimal design model' section above has the objective of minimising the compression member weight, given the constraints of the four main failure modes and manufacturing constraints. Here, a few aluminium alloy SHS compression members with different cross-sectional sizes were computed to interpret the optimisation scheme and the obtained results were then compared with those reported in the literature.

Comparison with existing experimental results

This section compares the optimal design results obtained by the present method with those reported in the literature (Su *et al* 2014), where the authors experimentally tested aluminium alloy SHS and RHS compression members with and without internal cross stiffeners.

In the previous study (Su *et al* 2014), specimens were first fabricated with special sizes, then compressed to obtain the failure loads. However, in the present comparison, the model was modified to design the sectional geometric properties of the compression members under the failure compression load tested by Su *et al* (2014), to obtain the minimum weight of the compression member. The weight of the optimal structure should be approximately equal to or less than those of the experimental specimens. Two cases of their study were executed. One axially compressed specimen is named as +H95×95×4.3C, which was made of high-strength aluminium alloy 6061-T6, and its nominal cross section with a cross internal stiffener had dimensions of 95 mm × 95 mm × 4.3 mm (wall thickness). Note that the thicknesses of the faces and stiffeners of the specimen were both 4.3 mm. The length of the specimens was 284.8 mm, and the failure load in the experiment was 585.6 kN. Hence, the aim is to obtain the optimal

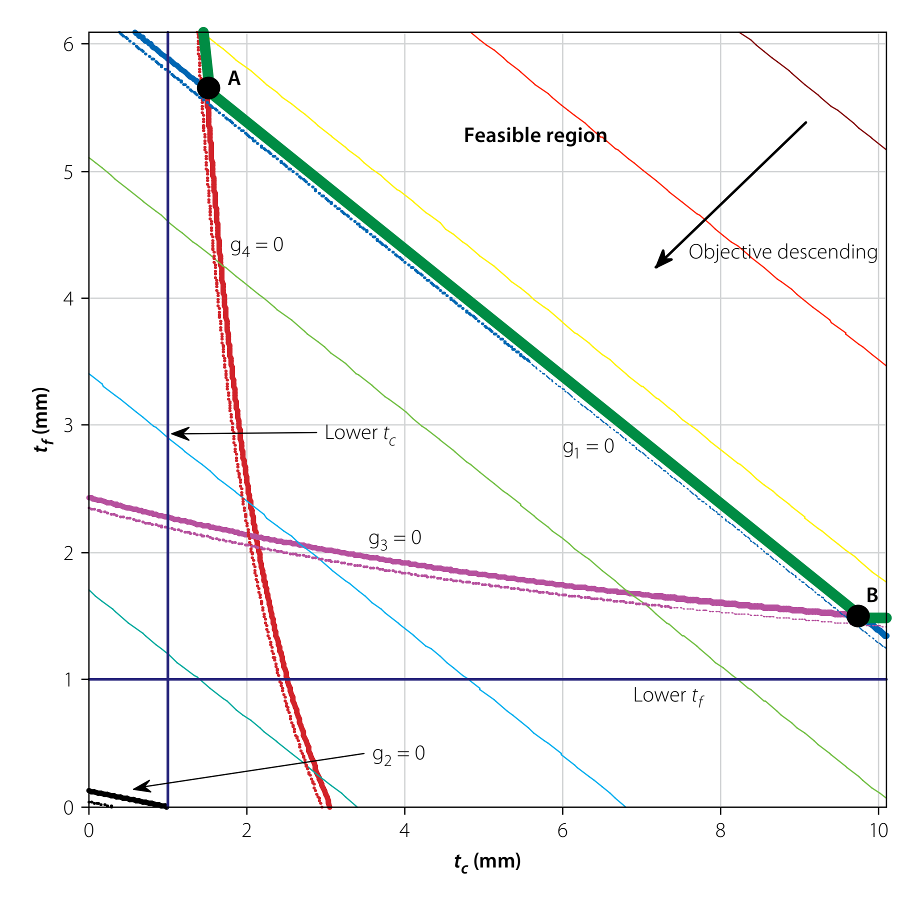

Figure 5 **Graphical solution of the optimal design of aluminium alloy SHS with cross sectional side length 95 mm and length 284.8 mm.**

thickness of this cross section with internal stiffeners to minimise the weight of the compression member. The other specimen used for comparison was H120×120×9.3C from the same study (Su *et al* 2014). The sketch of both sections is shown in Figure 4.

Note that the yielding stress in the optimisation formulation (Equation 17) must be replaced by the failure stress because the specimens under compression tested by Su *et al* (2014) significantly exceeded the yielding, hardening, and softening stages.

The graphic solution process is shown in Figure 5. This indicated that the dominant failure of the compression member is the yielding failure. In addition, there are an infinite number of optimal solutions because the contours of the objective function are parallel to the constraint function $g_1 = 0$, which represents the yielding failure mode of the compression members. Therefore, all points present on line AB represent optimal solutions. Introducing the same restriction as in Su *et al* (2014) – that the face thickness should be equal to the stiffener thickness – the optimal solution was obtained as $t_c = t_f = 4.26$ mm.

The present optimal design model is in good agreement with the experimental results. The thickness in the experiment was $t_c = t_f = 4.17$ mm, which is slightly thinner than the designed thickness. The relative difference between the designed and experimental thickness was only 2.16%. Moreover, the experimental thickness was one of the optimal thicknesses because the specimen actually failed in yielding (Su *et al* 2014).

Table 1 **Comparison between the optimal sections and the experimental ones from literature (Su *et al* 2014)**

Specimen	E (GPa)	σ_u (MPa)	P (kN)	H (mm)	L (mm)	t_{exp} (mm)	t_{opt} (mm)	Δ (%)
+H95×95×4.3C	67	240	585.6	95.4	284.8	4.17	4.26	2.16
H120×120×9.0C	65	234	981.5	120.0	360.2	8.91	8.74	1.91

Note: t_{exp} denotes the thickness of the specimen in experiments, t_{opt} denotes the thickness obtained in the optimisation formulation, $\Delta = |(t_{exp}-t_{opt})/t_{exp}| \times 100\%$

In addition, the specimen that was labelled as H120×120×9.3C with length 360.2 mm in the literature (Su *et al* 2014) was designed and compared, obtaining excellent agreement. Both cases with detailed parameters and comparison results are presented in Table 1.

As noted in the introduction, the similar load-bearing efficiency of compression members with and without stiffeners, as tested by Su *et al* (2014), can be explained by the optimisation model presented in this study. Because both compression members failed in yielding, their load-bearing capacity should be proportional to their cross-sectional areas, and as in Equation 1. Hence, their load-bearing efficiencies were very similar.

Optimal design of SHS compression members with section 150 mm × 150 mm

In this case, axial compression members with different slenderness ratios and the same cross-sectional size were considered. The compression members were made of 6061-T6 aluminium alloy, which has elastic modulus $E = 69$ GPa, Poisson's ratio $\nu = 0.3$, yielding stress or the 0.2% proof stress $\sigma_Y = 240$ MPa, and density $\rho = 2.7$ kg/mm^3 (The Aluminium Association 2020). All cross sections had fixed dimensions of $H \times H = 150$ mm × 150 mm, and the lengths were $L = 10H$, $20H$, and $30H$. For each case, the optimisation problems were solved based on the proposed optimal design model in the 'Optimal design model' section. The parameter n was set as 0 to 5 for each length. It should be noted that $n = 0$ indicates that there were no internal stiffeners at all; hence, the compression member was actually a square box sectional compression member. As mentioned in the 'Optimal design model' section, the lower bounds of t_f and t_c must be introduced to represent the manufacturing constraints; therefore, $\underline{t_f} = \underline{t_c} = 1$ mm was considered.

All the optimal results for SHS compression members with different lengths are listed in Table 2, which summarises the minimum weights, optimum thicknesses of the compression member walls and stiffeners, and the active constraints in the optimal solutions with different numbers of internal stiffeners. As the number of internal stiffeners increased, both the face wall and internal stiffener thicknesses decreased monotonically until the lower bounds were reached.

Quantitative analysis confirmed the considerable influence of the number of internal stiffeners on the minimum weight

Table 2 Optimal results versus cell sizes of the sandwich compression members at H = 150 mm

	n	t_c (mm)	t_f (mm)	AC	W (kg)	W*
L = 10H	0	0	3.19	g_3	7.56	1.00
	1	1.73	1.73	g_3, g_4	6.31	0.83
	2	1.19	1.19	g_3, g_4	5.78	0.76
	3	1.0	1.0	$\underline{t}_c$, $\underline{t}_f$	6.08	0.80
	4	1.0	1.0	$\underline{t}_c$, $\underline{t}_f$	7.29	0.96
L = 20H	0	0	3.11	g_3	15.11	1.00
	1	1.73	1.73	g_3, g_4	12.61	0.83
	2	1.19	1.19	g_3, g_4	11.57	0.77
	3	1.0	1.0	$\underline{t}_c$, $\underline{t}_f$	12.15	0.80
	4	1.0	1.0	$\underline{t}_c$, $\underline{t}_f$	14.58	0.96
L = 30H	0	0	3.11	g_3	22.67	1.00
	1	1.53	2.46	g_2, g_4	23.51	1.04
	2	1.02	2.3	g_2, g_4	24.2	1.07
	3	1.0	2.08	g_2, $\underline{t}_c$	26.1	1.15
	4	1.0	1.84	g_2, $\underline{t}_c$	27.99	1.23

Note: The meanings of the four constraints are provided in Equation 17; AC denotes active constraints; W* denotes the weight normalised by the weight of the member without stiffeners

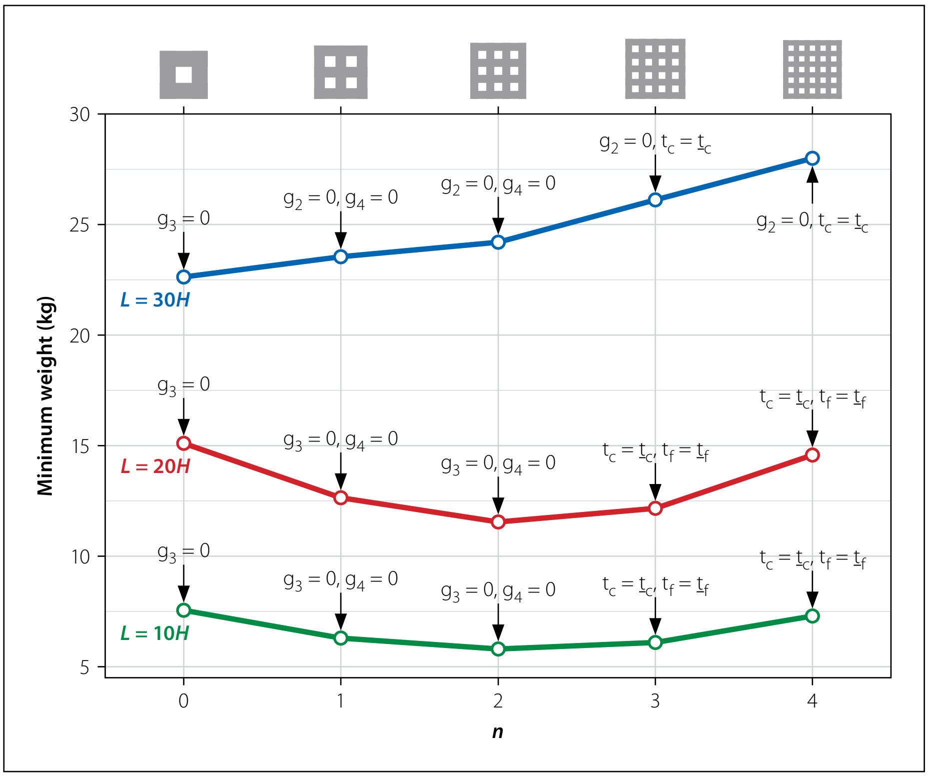

Figure 6 Optimal results versus numbers of internal stiffeners of compression members at H = 150 mm and L = 10H, 20H, and 30H. Labels denote the active constraints of the optimal solution at each case

of the SHS compression members more accurately. The minimum weight from n = 0 to n = 3 for a length of 10H decreased by as much as 24%. However, the minimum weight increased by as much as 23% for a compression member with length 30H from n = 0 to n = 4. This comparison is presented in Table 2, where the minimum weight with different numbers of internal stiffeners was normalised to that without any internal stiffener. Further, the most evident influence of the number of internal stiffeners on the minimum weight occurred between n = 0 and n = 1, that is, with and without stiffeners. At this stage, the minimum weight changed by more than 10% for L = 10H and 20H, and more than 5% for L = 30H.

The minimum weight and corresponding optimal t_f and t_c of the SHS compression members with different numbers of internal stiffeners are shown in Figure 6.

Figure 6 shows that the minimum weight of the SHS compression members exhibited a significant dependence on the number of internal stiffeners. This dependence showed different trends with respect to the compression member lengths. The minimum weight monotonically increased as n increased for compression members with length of 30H, while it decreased at the beginning and increased later for compression members with lengths of 20H and 10H. This particular phenomenon was caused by the different failure modes and activation of the lower size constraints on t_f and t_c. The member with a length of 30H is classified as a slender member. In contrast, those with lengths of 20H and 10H are considered short members. Consequently, a distinct difference in their failure modes is observed.

Moreover, when a compression member is prone to overall Euler buckling, its resistance fundamentally depends on achieving a high global moment of inertia (and thus bending stiffness). Consequently, for an SHS member under such conditions, a simple unstiffened box section generally represents the most efficient cross-sectional configuration. This case was verified by the curve L = 30H, as shown in Figure 6. However, if a compression member fails in simultaneous local buckling of the face walls and internal stiffeners, increasing the number of internal stiffeners is always an efficient way to improve the local buckling resistance of the compression member. This is because increasing the number of stiffeners results in a decreased width h of a local buckling panel and the corresponding critical buckling load is increased (see Equations 11 and 12). Further, minimum weight decreases monotonically at n = 0 – 2 for L = 10H and L = 20H, as shown in Figure 6. However, the monotonies of the minimum weight with respect to the number of internal stiffeners were often changed by the switch of the failure modes and activation of the size constraints owing to the manufacturing capacity (see L = 10H and 20H in Figure 6). This also indicates that it is difficult to find an optimal design for this type of structure using some simple rules provided in existing design codes.

The influence of the variation of size constraints was straightforward. This type of constraint always increased the minimum weight of compression members despite the failure modes because the number of stiffeners increased while the thickness of each stiffener remained unchanged (Figure 6). Hence, the minimum weights of the compression members increased for n = 3, where the size constraints were varied.

Optimal design of SHS compression members with section 120 mm × 120 mm

SHS compression members with section dimension of 120 mm × 120 mm were considered in this example. The material and computation procedures were the same as those in the previous example. The minimum weights of compression members with lengths L = 10H, 20H, and 30H and different numbers of internal stiffeners are shown in Figure 7.

The trends observed in this example were similar to those in the previous one. The significant influence of the number of internal stiffeners on the minimum weight of the SHS compression members was verified again.

All the optimal results for SHS compression members with different lengths are listed in Table 3, which summarises the minimum weight, optimum thicknesses of the compression member face thicknesses and stiffener thicknesses, and the active constraints at the optimal solutions with different numbers of internal stiffeners.

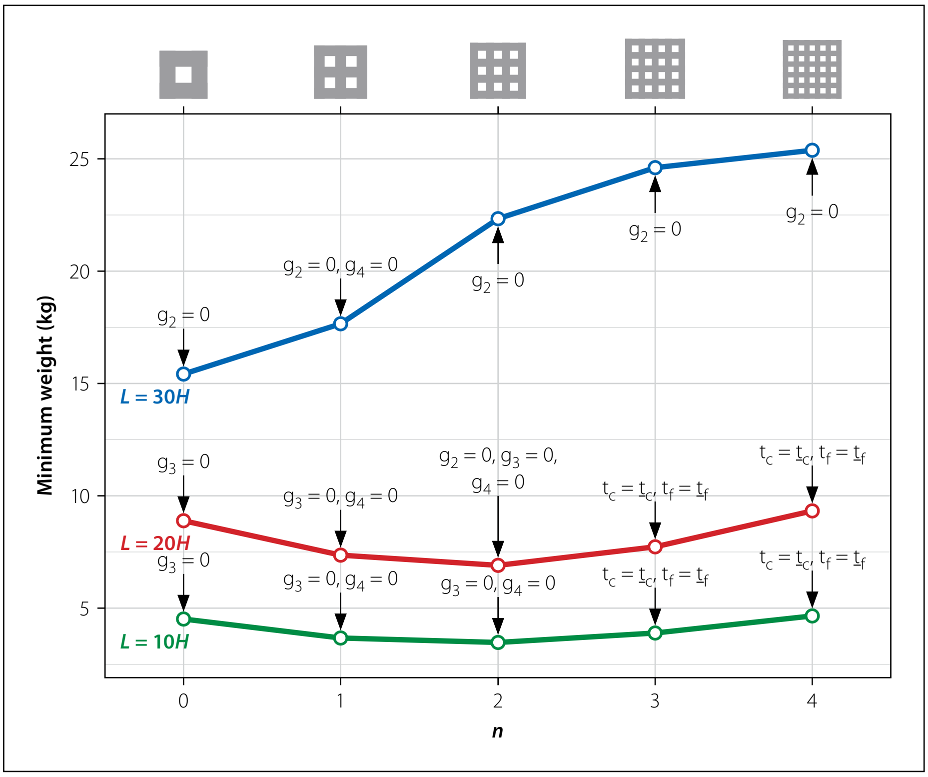

Figure 7 Optimal results versus numbers of internal stiffeners of compression members for H = 120 mm and L = 10H, 20H, and 30H

The trends observed for these quantities of optimal solutions were similar to those in the previous example.

Both examples confirmed the significant influence of the number of internal stiffeners on the minimum weight of aluminium alloy compression members with SHS. The monotonicity of the minimum weight with respect to the number of internal stiffeners was specified if the failure mode of the compression member was provided. As the number increased, the minimum weight decreased by more than 25% for compression members with local buckling failure, while it increased by more than 25% for compression members with overall buckling failure. The minimum weight remained unchanged as the number of stiffeners increased for compression members that failed in yielding. In addition, the failure mode often switched as the number of internal stiffeners increased. There always existed a minimum weight of compression member and an optimal finite number of internal stiffeners. This conclusion is satisfied even if the minimum weight monotonically decreased as the number increased because of the allowable lower thickness of the walls.

Table 3 Optimal results versus cell sizes of the sandwich compression members, H 120mm

	n	t_c (mm)	t_f (mm)	AC	W (kg)	W^*
L = 10H	0	0	2.89	g_3	4.49	1.00
	1	1.58	1.58	g_3, g_4	3.68	0.82
	2	1.12	1.12	g_3, g_4	3.48	0.78
	3	1.0	1.0	$\underline{t}_c, \underline{t}_f$	3.89	0.87
	4	1.0	1.0	$\underline{t}_c, \underline{t}_f$	4.67	1.04
L = 20H	0	0	2.89	g_3	8.98	1.00
	1	1.58	1.58	g_3, g_4	7.37	0.82
	2	1.11	1.11	g_2, g_3, g_4	6.91	0.77
	3	1.0	1.0	$\underline{t}_c, \underline{t}_f$	7.72	0.86
	4	1.0	1.0	$\underline{t}_c, \underline{t}_f$	9.33	1.04
L = 30H	0	0	3.3	g_2	15.41	1.00
	1	1.27	3.15	g_2, g_4	17.66	1.15
	2	2.22	2.57	g_2	22.35	1.45
	3	2.11	2.11	g_2	24.61	1.60
	4	1.78	1.88	g_2	25.38	1.65

CONCLUSIONS

This study proposed a simple and practical optimisation formulation for aluminium alloy axial compression members with SHS. The findings indicate that the number of internal stiffeners influence the load-bearing efficiency of compression members. The validity of the present optimal design formulation was confirmed through the experimental results, showing that this influence is significant. The main conclusions are summarised as follows:

- The optimum numbers of stiffeners differ with respect to the different failure modes of the axial compression

members. The optimum stiffener number is zero if a compression member fails in overall flexural buckling. The loading capacity is independent of the number of stiffeners if the compression member fails to yield. However, a non-zero stiffener number always exists if the compression member fails in the local buckling of the walls.
- The optimum thicknesses of the face and stiffener walls can be obtained by setting the active constraints as simultaneous equations after the failure modes of the compression member and number of stiffeners are determined.
- An optimal number of internal stiffeners exists to minimise the weight of a compression member under a given axial load. Utilising this optimum can achieve a weight reduction exceeding 20%.
- The failure mode of the compression member is influenced by the slenderness ratio of the member and the width-to-thickness ratios of the cross sections, which are influenced by the number of stiffeners.

This study widens the design scope of metal compression members under axial compression. The proposed method can be extended to compression members with other sectional shapes and engineering materials, such as steel. However, the right-hand sides of the constraint functions may be modified by safety factors and resistance factors for yielding and buckling constraints, respectively, in the design of engineering members. Moreover, for other members, torsional buckling and the torsional flexural buckling may be the main failure modes.

FUNDING

This work was supported by the National Natural Science Foundation of China (grant number 11902062) and the Foundation of Liaoning Province Education Administration (grant number LJ212510150020).

REFERENCES

Arora, J. 2017. *Introduction to optimum design*. 4th edn. Cambridge: Elsevier.

Budiansky, B. 1999. On the minimum weights of compression structures. *International Journal of Solids and Structures*, 36(24): 3677–3708.

Feng, R & Liu, J. 2019. Numerical investigation and design of perforated aluminium alloy SHS and RHS columns. *Engineering Structures*, 199:109591.

Feng, R, Mou, X, Chen, A & Ma, Y. 2016. Tests of aluminium alloy CHS columns with circular openings. *Thin-Walled Structures*, 109:113–131.

Feng, R, Mou, X, Chen, Z, Roy, K, Chen, B & Lim, J B P. 2020. Finite-element modelling and design guidelines for axial compressive capacity of aluminium alloy circular hollow sections with holes. *Thin-Walled Structures*, 157:107027.

Feng, R, Zhu, W, Wan, H, Chen, A & Chen, Y. 2018. Tests of perforated aluminium alloy SHSs and RHSs under axial compression *Thin-Walled Structures*, 130:194–212.

Georgantzia, E. 2021 Aluminium alloys as structural material: A review of research. *Engineering Structures*, 227:111372.

Jerath, S. 2020. *Structural Stability Theory and Practice: Buckling of Columns, Beams, Plates, and Shells.* 1st edn. Hoboken: John Wiley & Sons.

Liu, M, Zhang, L, Wang, P & Chang, Y. 2015a. Buckling behaviors of section aluminum alloy columns under axial compression. *Engineering Structures*, 95:127–137.

Liu, M, Zhang, L, Wang, P & Chang, Y. 2015b. Experimental investigation on local buckling behaviors of stiffened closed-section thin-walled aluminum alloy columns under compression. *Thin-Walled Structures*, 94:188–198.

Roux, W J, Stander, N & Snyman, J A. 1994. Conceptual design of rigidly framed structures using optimisation methods. *Journal of the South African Institution of Civil Engineers*, 36(2):9–14.

Su, M N, Young, B & Gardner, L. 2014. Testing and design of aluminum alloy cross sections in compression. *Journal of Structural Engineering*, 140(9):04014047.

Su, M N, Young, B & Gardner, L. 2017. Classification of aluminium alloy cross-sections. *Engineering Structures*, 141:29–40.

The Aluminium Association. 2020. *Aluminum Design Manual*. Arlington: The Aluminium Association.

Tian, Y S & Lu, T J. 2004. Minimum weight of cold-formed steel sections under compression. *Thin-Walled Structures*, 42(4):515–532.

Tian, Y S & Lu, T J. 2005. Optimal design of compression corrugated panels. *Thin-Walled Structures*, 43(3):477–498.

Timoshenko, S P & Gere, J M. 1963. *Theory of Elastic Stability*. 2nd edn. London: McGraw Hill.

Tsavdaridis, K D, Efthymiou, E, Adugu, A, Hughes, J A & Grekavicius, L. 2019. Application of structural topology optimisation in aluminium cross-sectional design. *Thin-Walled Structures*, 139:372–388.

Wang, Y Q, Wang, Z X, Hu, X G, Han, J K & Xing, H J. 2016. Experimental study and parametric analysis on the stability behavior of 7A04 high-strength aluminum alloy angle columns under axial compression. *Thin-Walled Structures*, 108:305–320.

Wang, Y Q, Yuan, H X, Chang, T, Du, X X & Yu, M. 2017. Compressive buckling strength of extruded aluminium alloy I-section columns with fixed-pinned end conditions. *Thin-Walled Structures*, 119:396–403.

Wang, Z X, Wang, Y Q, Sojeong, J & Ouyang, Y W. 2018. Experimental investigation and parametric analysis on overall buckling behavior of large-section aluminum alloy columns under axial compression. *Thin-Walled Structures*, 122:585–596.

Yu, W, LaBoube, R A & Chen, H. 2020. *Cold-formed steel design*. 5th edn. Hoboken: John Wiley & Sons.

Zhu, J H, Li, Z, Su, M N. & Young, B. 2019. Behaviour of aluminium alloy plain and lipped channel columns. *Thin-Walled Structures*, 135:306–316.